Solvent Effects on Heavy Atom Nuclear Spin−Spin Coupling Constants: A Theoretical Study of Hg−C and Pt−P Couplings

Jochen Autschbach* and Tom Ziegler*

Contribution from the Department of Chemistry, The University of Calgary, Alberta T2N 1N4, Canada

Received September 25, 2000. Revised Manuscript Received January 9, 2001

Abstract: The computation of indirect nuclear spin−spin coupling constants, based on the relativistic two-component zeroth order regular approximate Hamiltonian, has been recently implemented by us into the Amsterdam Density Functional program. Applications of the code for the calculation of one-bond metal−ligand couplings of coordinatively unsaturated compounds containing ^{195}Pt and ^{199}Hg, including spin−orbit coupling or coordination effects by solvent molecules, show that relativistic density functional calculations are able to reproduce the experimental findings with good accuracy for the systems under investigation. Spin−orbit effects are rather small for these cases, while coordination of the heavy atoms by solvent molecules has a great impact on the calculated couplings. Experimental trends for different solvents are reproduced. An orbital-based analysis of the solvent effect is presented. The scalar relativistic increase of the coupling constants is of the same order of magnitude as the nonrelativistically obtained values, making a relativistic treatment essential for obtaining quantitatively correct results. Solvent effects can be of similar importance.

1. Introduction

Nuclear magnetic resonance (NMR) spectroscopy is of great importance to gain experimental insight into the electronic and geometric structure of molecules. Additionally, theoretical methods may be used to compute the respective observables, such as shielding tensors and spin−spin coupling constants, from first principle quantum chemical theory. With the help of such calculations it is possible to get very detailed insight into the mechanisms which determine the experimental output, or to simulate NMR spectra to clarify experimental findings, propose data for yet unknown substances, etc. NMR parameters involving heavy nuclei such as ^{195}Pt, ^{199}Hg, or ^{207}Pb (see, e.g., refs 1−3) are of special interest but need an advanced theoretical treatment. It is known that a relativistic quantum mechanical formalism is necessary for a correct description of chemical bonding in heavy element systems. For sixth row elements, nonrelativistic calculations might yield even qualitatively wrong results.[4−8] NMR spin−spin couplings are determined by features of the valence orbitals very close to the nuclei,[9,12] and relativistic effects are quite substantial. No systematic quantitative agreement with experiment can generally be achieved by approximate methods based on atomic scaling factors (see, e.g., refs 13−18); therefore, a consistent relativistic treatment is desirable. The respective formalism and early molecular orbital (MO) and relativistic extended Hückel (REX) benchmark computations within the four-component Dirac picture were published by Pyykkö.[15,16] More recently, an implementation within the four-component Dirac−Hartree−Fock (DHF) method has been reported in refs 19 and 20. However, full four-component relativistic computations are computationally quite demanding, and the authors of ref 20 could also estimate that electron correlation will have a strong influence on the spin−spin couplings. Two-component relativistic density functional methods offer a promising route here to achieve reasonable accuracy at an affordable computational cost in order to obtain magnetic properties of larger heavy atom systems from first-principles theory.

The zeroth-order regular approximation (ZORA) method is an effective and transparent way in which to deal with relativistic effects of valence shells of heavy atom systems by means of a two-component variational approach.[21−24] In particular it has been shown that it is useful for the determination of magnetic properties such as NMR shieldings[25,26] and ESR **g** tensors.[27]

* Author correspondence. E-mail: jochen@cobalt78.chem.ucalgary.ca or ziegler@chem.ucalgary.ca.

(1) Wrackmeyer, B.; Horchler, K. *Annu. Rep. NMR Spectrosc.* **1989**, *22*, 249.
(2) Pregosin, P. *Annu. Rep. NMR Spectrosc.* **1986**, *17*, 285.
(3) Wrackmeyer, B.; Contreras, R. *Annu. Rep. NMR Spectrosc.* **1992**, *24*, 267.
(4) Pyykkö, P. *Chem. Rev.* **1988**, *88*, 563.
(5) Ziegler, T.; Snijders, J. G.; Baerends, E. J. *J. Chem. Phys.* **1981**, *74*, 1271.
(6) Snijders, J. G.; Pyykkö, P. *Chem. Phys. Lett.* **1980**, *75*, 5.
(7) Ziegler, T.; Snijders, J. G.; Baerends, E. *J. Chem. Phys. Lett.* **1980**, *75*, 1.
(8) Schwarz, W. H. E. In *The Concept of the Chemical Bond*; Masić, Z. B., Ed.; Springer: Berlin, 1990; Vol 2.
(9) Khandogin, J.; Ziegler, T. *Spectrochim. Acta* **1999**, *A55*, 607.
(10) Sychrovský, V.; Gräfenstein, J.; Cremer, D. *J. Chem. Phys.* **2000**, *113*, 3530.
(11) Helgaker, T.; Watson, M.; Handy, N. C. *J. Chem. Phys.* **2000**, *113*, 9402.
(12) Autschbach, J.; Ziegler, T. *J. Chem. Phys.* **2000**, *113*, 936.
(13) Pyykkö, P.; Pajanne, E. *Phys. Lett.* **1971**, *A35*, 53.
(14) Pyykkö, P,; Pajanne, E.; Inokuti, M. *Int. J. Quantum Chem.* **1973**, *7*, 785.
(15) Pyykkö, P. *Chem. Phys.* **1977**, *22*, 289.
(16) Pyykkö, P.; Wiesenfeld, L. *Mol. Phys.* **1981**, *43*, 557.
(17) Pyykkö, P. *Theor. Chem. Acc.* **2000**, *103*, 214.
(18) Khandogin, J.; Ziegler, T. *J. Phys. Chem.* **2000**, *A104*, 113.
(19) Visscher, L.; Enveldsen, T.; Saue, T.; Jensen, H. J. A.; Oddershede, J. *J. Comput. Chem.* **1999**, *20*, 1262.
(20) Enevoldsen, T.; Visscher, L.; Saue, T.; Jensen, H. J. A.; Oddershede, J. *J. Chem. Phys.* **2000**, *112*, 3493.
(21) Chang, C.; Pelissier, M.; Durand, M. *Phys. Scr.* **1986**, *34*, 394.
(22) van Lenthe, E.; Baerends, E. J.; Snijders, J. G. *J. Chem. Phys.* **1993**, *99*, 4597.
(23) van Lenthe, E.; Baerends, E. J.; Snijders, J. G. *J. Chem. Phys.* **1994**, *101*, 9783.
(24) van Lenthe, E.; van Leeuwen, R.; Baerends, E. J.; Snijders, J. G. *Int. J. Quantum Chem.* **1996**, *57*, 281.

10.1021/ja003481v CCC: $20.00
Published on Web 03/15/2001

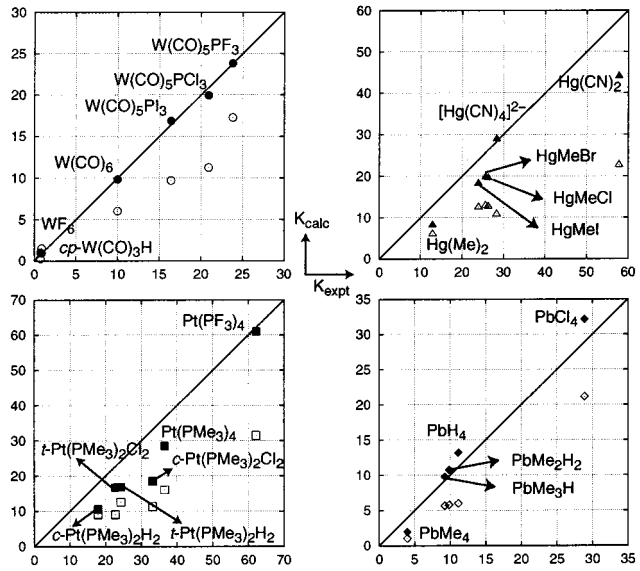

Figure 1. Comparison of density functional and experimental one-bond spin−spin couplings *K* for some sixth row element compounds. Figures based on data from ref 12 in 10^{21} kg m^{-2} C^{-2}. Filled markers denote scalar ZORA, open markers denote nonrelativistic results. Me = CH_3, *cp* = C_5H_5.

Recently it has been successfully applied by us to the density functional computation of one-bond NMR spin−spin coupling constants and anisotropies of heavy-atom systems.[12,28] That density functional theory (DFT) is able to predict nuclear spin−spin coupling constants with reasonable accuracy for a large range of light main-group element and transition-metal compounds has already been extensively demonstrated during the past decade.[9−11,29−33]

In our previous work[12,28] we have formulated the relevant operators arising from the ZORA magnetic hyperfine terms and described their implementation in the Amsterdam Density Functional (ADF) program.[34−36] We could show that scalar relativistic density functional calculations are able to reproduce experimental coupling constants with good accuracy for a variety of systems containing W, Pt, Hg, and Pb. Figure 1 displays scalar ZORA couplings in comparison with experiment for the compounds studied by us in ref 12. In particular for the tungsten and partially for the lead couplings almost quantitative agreement with experimental data is obtained. Except for WF_6 and $Pb(CH_3)_4$, the coupling in those systems is almost exclusively determined by the well-known Fermi-contact term and the scalar relativistic effects on this contribution (see section 2 for a description of the individual contributions to the coupling constants). Electron correlation is very important in order to obtain good estimates of spin−spin couplings, which is to some extent accounted for by standard Kohn−Sham density functionals, while the Dirac−Hartree−Fock approach seems to perform much less accurately, at least for plumbanes.[20,28]

The spin−dipole contribution, which has been omitted in pioneering DFT studies of spin−spin couplings,[30,32,33] is available with our code (nonrelativistic and its ZORA generalization) and can be all but negligible for certain systems, as has been shown in particular for the X−F (X = Cl, Br, I) couplings in ref 28, in agreement with the correlated ab initio study of ClF in ref 37. See also refs 10 and 11 for recent nonrelativistic DFT implementations of spin−spin couplings including the spin-dipole term.

Recalling that for the Hg and Pt compounds in Figure 1 the only important contribution is due to the Fermi-contact term, one might expect, when comparing to experiment, an accuracy similar to that for for the W (or Pb) compounds. From Figure 1, however, it becomes obvious that too small coupling constants are systematically obtained, in particular for the linear $Hg(CN)_2$ and $H_3C-Hg-X$ (X = CH_3, Cl, Br, I) and the square planar $PtX_2(P(CH_3)_3)_2$ (X = H, Cl) complexes, a result which was speculatively attributed by us[12] to the neglect of spin−orbit coupling and of the spin-dipole term, or to the influence of solvent molecules, since the experimental data were obtained in solution. In ref 28 we could show that the spin-dipole term is, for example, negligible for the plumbanes, while rather small spin−orbit effects correct for the slight overestimation of the Pb−H couplings in comparison with experiment. On the other hand, it has already been shown in ref 38 that even if a solvent is treated only implicitly as a polarizable dielectric continuum, its effects on the spin−spin couplings are not negligible. See also, for example, ref 39. Since those Hg and Pt systems mentioned above are not coordinatively saturated, solvent molecules may coordinate to the heavy atom. This will not be (or will be much less) the case for tetrahedral or octahedral systems such as the W and Pb compounds from Figure 1, for which the scalar ZORA coupling constants for the free molecules already agree quite satisfactorily with experiment.

The aim of this work is to demonstrate that good agreement with experimental data for the one-bond metal−ligand NMR spin−spin coupling constants for $Hg(CN)_2$, $H_3C-Hg-X$ and $PtX_2(P(CH_3)_3)_2$ can be achieved by ZORA relativistic density functional computations with explicit accounting for coordination of the heavy atom by solvent molecules. We will show that the spin−orbit effects on the coupling constants as well as the spin-dipole contributions are small compared to the solvent effects and can rather be neglected for our samples at the present level of accuracy. From an analysis of the solvent coordination effect in terms of individual orbital contributions we will conclude that it is mostly due to charge donation from solvent lone pairs to the heavy metal, which is not accounted for if the solvent is only implicitly treated as a polarizable continuum.

In section 2 we briefly recall the main features of the formalism presented in refs 12 and 28. Section 3 deals with computational details, while results for $Hg(CN)_2$, H_3C-Hg-

(25) (a) Wolff, S. K.; Ziegler, T.; van Lenthe, E.; Baerends, E. J. *J. Chem. Phys.* **1999**, *110*, 768. (b) Schreckenbach, G.; Wolff, S. K.; Ziegler, T. In *Modeling NMR Chemical Shifts*; Facelli, J. C., de Dios, A., Eds.; ACS Symposium Series; American Chemical Society: Washington DC, 1999.
(26) Gilbert, T.; Ziegler, T. *J. Phys. Chem.* **1999**, *A103*, 7535.
(27) van Lenthe, E.; van der Avoird, A.; Wormer, P. E. S. *J. Chem. Phys.* **1998**, *108*, 4783.
(28) Autschbach, J.; Ziegler, T. *J. Chem. Phys.* **2000**, *113*, 9410.
(29) Helgaker, T.; Jaszuński, M.; Ruud, K. *Chem. Rev.* **1999**, *99*, 293.
(30) Malkin, V. G.; Malkina, O. L.; Salahub, D. R. *Chem. Phys. Lett.* **1994**, *221*, 91.
(31) Malkin, V. G.; Malkina, O. L.; Eriksson, L. A.; Salahub, D. R. In *Modern Density Functional Theory: A Tool for Chemistry*; Politzer, P., Seminario, J. M., Eds.; Elsevier: Amsterdam, 1995.
(32) Malkina, O. L.; Salahub, D. R.; Malkin, V. G. *J. Chem. Phys.* **1996**, *105*, 8793.
(33) Dickson, R. M.; Ziegler, T. *J. Phys. Chem.* **1996**, *100*, 5286.
(34) Baerends, E. J.; Ellis, D. E.; Ros, P. *Chem. Phys.* **1973**, *2*, 41.
(35) Baerends, E. J.; Ros, P. *Chem. Phys.* **1973**, *2*, 52.
(36) ADF 2.3.3, Theoretical Chemistry, Vrije Universiteit: Amsterdam. ADF 1999.02, Theoretical Chemistry, Vrije Universiteit: Amsterdam. http://www.scm.com. See also: te Velde, G.; Baerends, E. J. *J. Comput. Phys.* **1992**, *99*, 84; Fonseca Guerra, C.; Visser, O.; Snijders, J. G.; te Velde, G.; Baerends, E. J. In *Methods and Techniques for Computational Chemistry*; Clementi, E., Corongiu, C., Eds.; STEF: Cagliari, 1995, p. 303.
(37) Bryce, D. L.; Wasylishen, R. *J. Am. Chem. Soc.* **2000**, *122*, 3197.
(38) Mikkelsen, K. V.; Ruud, K.; Helgaker, T. *J. Comput. Chem.* **1999**, *20*, 1281.
(39) Pecul, M.; Sadlej, J. *Chem. Phys.* **1998**, *234*, 111.

X, and $PtX_2(P(CH_3)_3)_2$ are reported and discussed in section 4. Concluding remarks are given in section 5.

2. Methodology

This work deals with the *indirect* nuclear spin−spin coupling constants, that is, the effect of the presence of a pair of nuclear magnetic dipoles on the molecular energy due to their interaction with the electrons. For freely and rapidly rotating molecules, for example in the case of measurements carried out in gas phase or solution, the direct coupling between the nuclei does not yield a net contribution to the spin−spin coupling. We will refer to the indirect couplings throughout this paper when speaking about spin−spin coupling constants.

The so-called reduced NMR spin−spin coupling constant K(A,B) involving two magnetically active nuclei A, B with nuclear magnetic moments $\mu_A = \gamma_A \boldsymbol{I}_A$ etc. is obtained from the total (relativistic) energy E of the system by

$$K_{jk}(\mathrm{A,B}) = \left.\frac{\partial^2 E}{\partial \mu_{\mathrm{A}j}\partial \mu_{\mathrm{B}k}}\right|_{\mu_{\mathrm{A}j}=0,\mu_{\mathrm{B}k}=0} \tag{1}$$

The $\boldsymbol{I}$'s are the intrinsic angular momenta of the nuclei, the γ's the nuclear magneto-gyric ratios, and $j,k \in \{x,y,z\}$. The reduced coupling constant is the isotropic part $K = (1/3)(K_{xx} + K_{yy} + K_{zz})$ of the $\mathbf{K}$ tensor. Experimentally observed are the coupling constants J(A,B) in Hertz:

$$J(\mathrm{A,B}) = \frac{h}{4\pi^2}\gamma_A\gamma_B K(\mathrm{A,B}) \tag{2}$$

Within Kohn−Sham DFT we compute the second derivative of the energy by double perturbation theory,[40] the φ_i being the singly occupied one- or two-component Kohn−Sham orbitals:

$$K_{jk}(\mathrm{A,B}) = \sum_i^{\mathrm{occ}} \langle \varphi_i^{(0,0)} | \hat{H}^{(\mu_{\mathrm{A}j},\mu_{\mathrm{B}k})} | \varphi_i^{(0,0)} \rangle + 2\mathrm{Re}\langle \varphi_i^{(0,0)} | \hat{H}^{(\mu_{\mathrm{A}j},0)} | \varphi_i^{(0,\mu_{\mathrm{B}k})} \rangle \tag{3}$$

The superscripts $(\mu_{Aj},0)$, etc. denote the order of perturbation with respect to the perturbation parameters μ_{Aj} and μ_{Bk}. In ref 12 we have derived the respective perturbation operators for the ZORA Hamiltonian and obtained the following three contributions (in atomic units with $h = 2\pi$, $e = 1$, $m_e = 1$, $4\pi\epsilon_0 = 1$, $c \approx 137.036$):

1. The ZORA diamagnetic orbital (DSO) term

$$\hat{H}^{(\mu_{\mathrm{A}j},\mu_{\mathrm{B}k})}_{\mathrm{ZDSO}} = \frac{K}{c^4}\frac{\delta_{jk}(\mathbf{r}_A\cdot\mathbf{r}_B) - r_{Ak}r_{Bj}}{r_A^3 r_B^3} \tag{4a}$$

2. the ZORA paramagnetic orbital (PSO) term

$$2c^2 i\cdot\hat{H}^{(\mu_{\mathrm{A}j},0)}_{\mathrm{ZPSO}} = \frac{K}{r_A^3}(\boldsymbol{r}_A \times \vec{\nabla})_j + (\boldsymbol{r}_A \times \vec{\nabla})_j\frac{K}{r_A^3} \tag{4b}$$

3. and the ZORA spin term (FC + SD)

$$2c^2\cdot\hat{H}^{(\mu_{\mathrm{A}j},0)}_{\mathrm{ZSO}} = \sigma_j\vec{\nabla}\left(K\frac{\boldsymbol{r}_A}{r_A^3}\right) - \boldsymbol{\sigma}\nabla_j\left(K\frac{\boldsymbol{r}_A}{r_A^3}\right) \tag{4c}$$

with $K = 2c^2/(2c^2 - V)$, V being the molecular Kohn−Sham potential. $\boldsymbol{r}_A$ is the electronic coordinate with respect to nucleus A, and $r_A = |\boldsymbol{r}_A|$. Further, $\boldsymbol{\sigma}$ represents the 3-vector of the standard Pauli spin matrices.

The nonrelativistic theory of nuclear spin−spin couplings has been formulated by Ramsey in 1953.[41] In eqs 4a−4c the nonrelativistic limit is achieved by letting $K \to 1$, thereby obtaining the sum of the well-known Fermi-contact (FC) and spin−dipole (SD) terms of Ramsey's theory from eq 4c after carrying out the differentiations, while the diamagnetic (DSO) and paramagnetic (PSO) orbital terms are obtained from eqs 4a and 4b, respectively. The acronyms DSO and PSO refer to "diamagnetic spin−orbit" etc. which are often used in the literature. However, we want to avoid "spin−orbit" (i.e., nuclear-spin−electron-orbit) in their names in order not to confuse it with relativistic spin−orbit (i.e., electron-spin−same-electron-orbit) coupling effects, see below. The diagonal part of eq 4c,

$$\hat{H}^{(\mu_{\mathrm{A}j},0)}_{\mathrm{ZSO-FC}} = \frac{1}{3c^2}\sigma_j\vec{\nabla}\left(K\frac{\boldsymbol{r}_A}{r_A^3}\right) \tag{5}$$

corresponds to the Fermi contact operator alone in the nonrelativistic limit and was used together with eqs 4a and 4b for the scalar relativistic computations in ref 12, while the remaining part of eq 4c, corresponding to the spin−dipole term, was neglected.

To take full advantage of the ZORA relativistic approach, we have recently implemented the computation of the SD part of the matrix elements of eq 4c, and extended our program to base its calculations on (generally complex) two-component spin−orbit coupled ZORA Kohn−Sham orbitals. The details are described elsewhere.[28] For simplicity we will refer to "Fermi-contact" (FC) and "spin−dipole" (SD) as well as "paramagnetic" (PSO) and "diamagnetic" (DSO) "orbital" terms also when we discuss their ZORA generalizations.

The DSO/PSO and FC/SD coupling mechanisms originate from the interaction of the nuclear spins with the electronic orbital and spin magnetic moments, respectively. If the electrons are treated relativistically, coupling of electronic spin and orbital angular momentum results in cross terms between the DSO/PSO and FC/SD nuclear spin−spin coupling mechanisms, of which the FC−PSO cross term was found to be the most important one in a number of systems.[28,42] For sixth row element compounds, spin−orbit coupling can often be neglected to lowest order, resulting in a so-called scalar relativistic treatment. This approach has, for example, been used[12] to obtain the data presented in Figure 1.

In ref 28 we could demonstrate that spin−orbit effects have a strong impact on the Tl−X (X = F, Cl, Br, I) couplings, where they can yield the most important contributions. See Table 1. For these systems, scalar relativistic computations result in unreasonably small magnitudes of the couplings. Especially the case of TlI is seen to be quite spectacular. Note that the spin−orbit effects on the PSO contribution are of the same order of magnitude as the (FC+SD) × PSO cross terms in TlX. We refer to ref 28 for a more detailed discussion.

Since a dominant contribution to the Tl−X couplings is due to the paramagnetic orbital (PSO) term, while the total coupling—especially in TlI—is determined by cancellation of contributions of different signs, the overall accuracy of the DFT results is not as good as for the octahedral W and tetrahedral Pb compounds in Figure 1. As already mentioned above, for most of these systems in Figure 1 the FC term

Table 1. Reduced Spin−Spin Coupling Constants K for TlX (X = F, Cl, Br, I) from Density Functional Computations,[28,a] in 10^{20} kg m^{-2} C^{-2}

	TlF	TlCl	TlBr	TlI
nrel LDA	−124.1	−136.4	−219.2	−288.5
nrel GGA	−120.3	−133.2	−217.2	−287.8
scalar LDA	−139.7	−124.7	−122.0	−88.2
scalar GGA	−138.8	−128.8	−131.6	−114.9
so LDA[b]	−208.6	−225.2	−320.6	−385.3
	(−42.0)	(−63.1)	(−126.0)	(−189.8)
so GGA[b]	−203.4	−218.5	−315.3	−381.8
	(−39.2)	(−56.9)	(−114.9)	(−169.8)
expt.[c]	−202	−224	−361	−474

[a] See also section 3. "nrel" refers to nonrelativistic, "scalar" to scalar relativistic ZORA, "so" to ZORA spin−orbit computations. [b] Values in parentheses refer to the (FC+SD) × PSO relativistic cross terms due to spin−orbit coupling. This does not include the spin−orbit effects on the individual terms itself. Compare ref 28. [c] Experimental estimates from ref 37.

(40) Epstein, S. T. *The Variation Method in Quantum Chemistry*; Academic Press: New York, 1974.

(41) Ramsey, N. F. *Phys. Rev.* **1953**, *91*, 303.

(42) (a) Kirpekar, S.; Sauer, S. P. A. *Theor. Chem. Acc.* **1999**, *103*, 146. (b) Kirpekar, S.; Jensen, H. J. A.; Oddershede, J. *Theor. Chim. Acta* **1997**, *95*, 35.

yields the only non-negligible contribution. It has been reported earlier that standard LDA or GGA density functionals together with Slater basis sets lead to less accurate results if the PSO term is large, since it is often overestimated in magnitude by DFT,[9,18,33] while the FC contribution seems to be less problematic. We are currently investigating inaccuracies of computed DFT magnetic properties caused by certain approximations in the density functionals.[43]

3. Computational Details

All computations were performed with the Amsterdam Density Functional (ADF) package,[36] using the ZORA[22−24] relativistic method. The Vosko−Wilk−Nusair (VWN)[44] density functional (local density approximation, LDA) was applied to determine the unperturbed molecular orbitals, while the Xα method[45] has been used for the determination of the first-order exchange potential due to the perturbation operators. From the computational results of ref 12 it could not be decided whether use of density-gradient corrected (GGA) functionals (as, e.g., described in refs 46 and 47) for the determination of the zeroth order orbitals or in the coupled perturbed Kohn−Sham procedure improves the couplings compared to experiment. From the investigations in ref 28 it seems that GGA functionals improve the coupling tensors significantly for systems where the PSO term dominates, while LDA and GGA yield quite similar results for compounds where all but the FC contributions are negligible. We have therefore restricted this work to the use of the VWN density functional, since the coupling in the investigated Hg and Pt complexes is controlled by the FC mechanism.

The ZORA spin−spin coupling calculations were carried out with the triple-ζ +pol. valence/double-ζ core all-electron Slater basis sets augmented with tight s-functions as described in refs 12 and 28. For the solvated Pt complexes, frozen cores were used for the solvent molecules and the carbons of the phosphine ligands, using the ADF frozen core ZORA basis sets IV, see ref 36. Fully optimized geometries for the solvated molecules were obtained from quasi-relativistic ADF computations[48,49] using the frozen-core ADF basis sets IV with smallest frozen cores (including, e.g., 4f, 5spd, and 6s as valence shells for Hg and Pt). Experimental geometries were used for the free molecules. The structural data was taken from ref 50 for $Hg(CH_3)_2$, from ref 51 for $Hg(CH)_3X$, from ref 52 for $Hg(CN)_2$, from ref 53 for the platinum hydride, and from ref 54 for the platinum chloride complexes.

Isosurface plots of molecular Kohn−Sham orbitals have been prepared with the ADFPLT program which is available from one of the authors (J.A.) upon request. Isosurface values are ± 0.03 atomic units, that is, $\pm 0.03\sqrt{\text{electrons/bohr}^3}$ (1 bohr ≈ 0.529 Å).

(43) Patchkovskii, S.; Autschbach, J.; Ziegler, T. *J. Chem. Phys.* Manuscript submitted.
(44) Vosko, S. H.; Wilk, L.; Nusair, M. *Can. J. Phys.* **1989**, *58*, 1200.
(45) Slater, J. C. *Phys. Rev.* **1951**, *81*, 385.
(46) Becke, A. D. *Phys. Rev.* **1988**, *A38*, 3098.
(47) Perdew, J. P. *Phys. Rev.* **1986**, *B33*, 8822. Erratum: *Phys. Rev.* **1986**, *B34*, 7406.
(48) Ziegler, T.; Tschinke, V.; Baerends, E. J.; Snijders, J. G.; Ravenek, W. *J. Phys. Chem.* **1989**, *93*, 3050.
(49) Schreckenbach, G.; Ziegler, T.; Li, J. *Int. J. Quantum Chem.* **1995**, *56*, 477.
(50) Kashiwabara, K.; Konaka, S.; Ijima, T.; Kimura, M. *Bull. Chem. Soc. Jpn.* **1973**, *46*, 407.
(51) Wallis, C.; Lister, D. G.; Sheridan, J. *J. Chem. Soc., Faraday Trans. 2* **1975**, *71*, 1091.
(52) Åkesson, R.; Persson, I.; Sandström, M.; Wahlgren, U. *Inorg. Chem.* **1994**, *33*, 3715.
(53) Packett, D. L.; Jensen, C. M.; Cowan, R. L.; Strouse, C. E.; Trogler, W. C. *Inorg. Chem.* **1985**, *24*, 3578.
(54) Hitchcock, P. B.; Jacobson, B.; Pidcock, A. J. *Organomet. Chem.* **1977**, *136*, 397.

Table 2. Computed One-Bond Hg−C Spin−Spin Couplings *K* for the Unsolvated Systems HgMeX (Me = CH_3, X = Me, Cl, Br, I) and $Hg(CN)_2$, in 10^{20} kg m^{-2} C^{-2} [a]

	HgMeCl	HgMeBr	HgMeI	$HgMe_2$	$Hg(CN)_2$
			nonrelativistic		
PSO	−0.8	−0.9	−1.2	−2.7	−0.3
FC	123.0	125.2	121.1	60.9	238.2
SD	−0.3	−0.3	−0.3	0.1	0.1
total *K*	122.0	124.0	119.5	58.2	237.9
			scalar ZORA		
PSO	0.3	0.1	−0.2	−2.8	−0.8
FC	183.7	185.9	177.6	77.2	444.0
SD	0.0	−0.1	−0.2	0.3	0.1
total *K*	184.0	185.9	177.2	74.8	443.4
			spin−orbit ZORA		
PSO	−0.5	−0.7	−1.2	−3.9	−1.4
FC	180.4	182.9	174.0	78.2	443.7
SD	−0.8	−1.0	−1.2	−0.7	−2.2
(FC+SD) × PSO[b]	−7.7	−7.9	−8.2	−9.9	−14.6
total *K*	171.4	173.4	163.4	63.8	425.5
expt.[c]	263.1[d]	256.3[d]	239.3[d]	126.6[d]	577.8[e]

[a] See sections 3 and 4.1. The DSO contributions are smaller than 0.1×10^{20} kg m^{-2} C^{-2} and therefore not displayed. [b] FC+SD × PSO refers to the relativistic cross terms due to spin−orbit coupling. [c] Experimental data obtained in solution [d] In $CDCl_3$, ref 55. [e] In MeOH, ref 56.

Table 3. Computed One-Bond Pt−P Spin−Spin Couplings *K* for the Unsolvated Systems *cis*- and *trans*-Ptϕ_2X_2 (ϕ = PMe_3, Me = CH_3, X = H, Cl), in 10^{20} kg m^{-2} C^{-2} [a]

	c-Ptϕ_2H_2	*t*-Ptϕ_2H_2	*c*-Ptϕ_2Cl_2	*t*-Ptϕ_2Cl_2
		nonrelativistic		
PSO	−1.9	−3.5	−4.7	−2.0
FC	91.5	130.0	163.5	93.2
SD	2.1	1.5	0.6	1.8
total *K*	91.7	128.1	159.4	93.1
		scalar ZORA		
PSO	−4.2	−6.0	−7.8	−3.7
FC	108.8	173.2	267.3	165.8
SD	2.4	2.0	1.3	2.4
total *K*	107.0	169.2	260.9	164.6
		spin−orbit ZORA		
PSO	−4.5	−6.3	−7.9	−3.7
FC	110.8	172.7	267.8	168.8
SD	1.4	1.1	0.1	1.6
(FC+SD) × PSO[b]	−10.5	−5.5	5.6	−3.5
total *K*	97.2	162.0	265.6	163.2
expt.[c]	178.7[d]	247.2[d]	331.6[e]	226.7[e]

[a] See sections 3 and 4.1. The DSO contributions are smaller than 0.1×10^{20} kg m^{-2} C^{-2} and therefore not displayed. [b] FC+SD × PSO refers to the relativistic cross terms due to spin−orbit coupling. [c] Experimental data obtained in solution. [d] In acetone-d_6, refs 57 and 58. [e] In CH_2Cl_2, ref 59.

4. Results

4.1. Unsolvated Compounds, General Remarks. In Tables 2 and 3, relativistically and nonrelativistically computed one-bond Hg−C and Pt−P spin−spin coupling constants for the unsolvated HgMeX (Me = CH_3, X = Me, Cl, Br, I), $Hg(CN)_2$, and *cis*- and *trans*-Ptϕ_2X_2 (ϕ = PMe_3, X = H, Cl) are displayed.

The coupling constants are systematically too small compared to experiment. In all of the investigated systems the DSO contribution (due to eq 4a) to the couplings is almost completely negligible, that is, smaller than 0.1×10^{20} kg m^{-2} C^{-2}, while the observed couplings are of the order of magnitude $10^2 \times 10^{20}$ kg m^{-2} C^{-2}. Furthermore, the PSO contribution due to eq 4b is small ($\sim 1 \times 10^{20}$ kg m^{-2} C^{-2}), while the ZSO term (eq 4c), or precisely its FC part (5), yields by far the most important

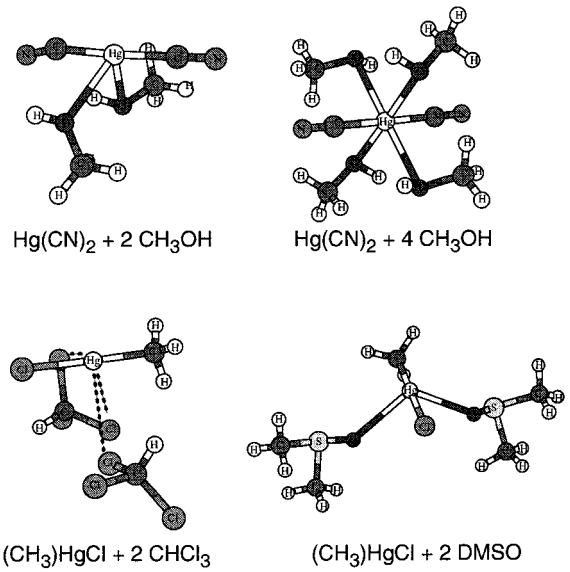

Figure 2. Some examples of structures of solvated Hg compounds obtained from ADF quasirelativistic geometry optimizations. See sections 3 and 4.2.

contribution to the coupling constants. Our samples are therefore rather "classic" in the sense that the coupling is almost exclusively determined by the FC mechanism. In experimental work interpretations of the observed coupling constants are often based on the respective nonrelativistic expression of the FC contribution within a simple MO picture,[60] as for example in ref 55 concerning solvent effects on Hg−C couplings.

The SD operator contributes to the isotropic coupling constant, as it is known from the nonrelativistic formalism, but its contribution is often small. However, counter examples are known, see for example refs 28, 37, 61, and 62. We find that for the investigated systems the SD contribution is indeed very small ($\sim 1 \times 10^{20}$ kg m^{-2} C^{-2}). Spin−orbit effects are of magnitude 10×10^{20} kg m^{-2} C^{-2} and therefore not negligible. However, because of the dominance of the FC term in our samples, we will not list the individual contributions to the coupling constants for the solvated complexes in the next paragraph and also omit the expensive computation of the SD term and spin−orbit effects in most cases.

The relativistic effects on the couplings are very large; see also Figure 1. The relativistic increase of coupling constants involving Hg and a light atom is typically of the same order of magnitude as the nonrelativistically obtained results. In cases where the coupling is due to the FC term only, this effect can often be computed with reasonable accuracy just by scaling the nonrelativistic orbital contributions with factors obtained from relativistic atomic calculations.[14,18,63] Such a scaling fails, however, if the bonding situation changes due to relativity, and the individual contributions of orbitals to the bonds are very different as compared to the nonrelativistic case. See section 4.2 for an example.

(55) Brown, A. J.; Howarth, O. W.; Moore, P. *J. Chem. Soc., Dalton Trans.* **1976**, 1589.
(56) Sebald, A.; Wrackmeyer, B. *J. Magn. Res.* **1985**, *63*, 397.
(57) Paonessa, R. S.; Trogler, W. C. *J. Am. Chem. Soc.* **1982**, *104*, 1138.
(58) Paonessa, R. S.; Trogler, W. C. *Inorg. Chem.* **1983**, *22*, 1038.
(59) Goggin, P, L.; Goodfellow, R. J.; Haddock, S. R.; Knight, J. R.; Reed, F. J. S.; Taylor, B. F. *J. Chem. Soc.* **1974**, 523.
(60) Pople, J. A.; Santry, D. P. *Mol. Phys.* **1964**, *8*, 1.
(61) Kowalewski, J. *Annu. Rep. NMR Spectrosc.* **1982**, *12*, 81.
(62) Kaski, J.; Lantto, P.; Vaara, J.; Jokisaari, J. *J. Am. Chem. Soc.* **1998**, *120*, 3993.
(63) Breit, G. *Phys. Rev.* **1930**, *35*, 1447.

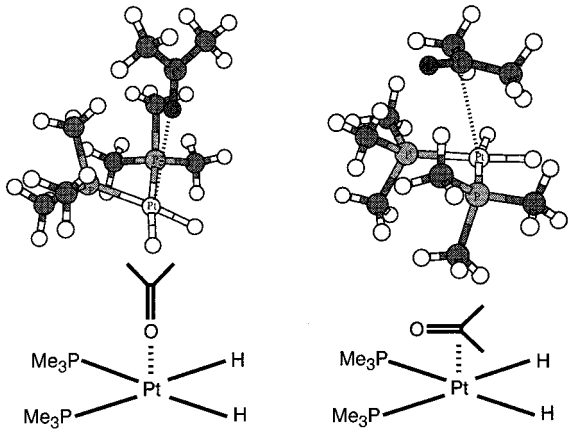

Figure 3. Different ways of coordinating acetone to *cis*-Pt(P(CH$_3$)$_3$)$_2$H$_2$, from ADF quasirelativistic geometry optimizations. See sections 3 and 4.2. Left figure = perpendicular (⊥) arrangement, right figure = parallel (∥) arrangement.

Table 4. Computed Hg−C One-Bond Spin−Spin Couplings K for the Solvated Compounds HgMeX (Me = CH$_3$, X = Me, Cl, Br, I) and Hg(CN)$_2$, in 10^{20} kg m^{-2} C^{-2}

cmpd	solvent	+ 2 solv.[a,b]	+ 3 solv.[a,b]	+ 4 solv.[a,b]	expt.	$\bar{R}$[c]
HgMeCl	$CHCl_3$	223.5	233.5	277.1 261.5[e]	263.1[h]	3.25
	DMSO	260.3	295.2		307.8[h]	2.65[f]
HgMeBr	$CHCl_3$	218.9	227.2		256.3[h]	3.28
	DMSO	253.8	293.6		299.9[h]	2.69[f]
HgMeI	$CHCl_3$	192.9	241.2		239.3[h]	3.28
	DMSO	251.0	295.4		283.1[h]	2.66[f]
$HgMe_2$[d]	$CHCl_3$	108.0	121.8		126.6[h]	3.28
	DMSO	118.5	130.7		133.4[h]	2.89
$Hg(CN)_2$[d]	MeOH	513.1		576.2 560.7[e]	577.8[i]	2.59[g]
	THF	511.5		581.8	558.5[j]	2.58[g]

[a] Coupling constant including the number of specified solvent molecules. [b] Scalar ZORA: FC + PSO + DSO coupling. [c] Mean distance between the heavy metal and the closest O or Cl solvent atoms in Å. [d] Mean value of both Hg−C coupling constants. [e] ZORA spin−orbit computation including the SD term. [f] For three DMSO. One DMSO is at a distance of ~3.5 Å. [g] For two solvents. With four solvents the distances are 2.67 Å for MeOH and 2.68 Å for THF, respectively. [h] Reference 55. [i] Reference 56. [j] Reference 64.

4.2. Solvent Effects on the Spin−Spin Coupling Constants. Experimental data for the investigated Hg and Pt compounds have been obtained in solution. Geometry optimizations for the complexes including up to four solvent molecules coordinating to the heavy atom were carried out with the ADF program. See section 3 for details. Figures 2 and 3 display some of the structures that have been obtained. Since spin−orbit computations on the solvated complexes are very expensive, we have carried out such spin−spin coupling calculations (including the SD contribution) only for a few examples. The rather small spin−orbit corrections do not change very much due to solvation as compared to the solvent shift of the FC contribution. The very small SD contribution has been neglected in the scalar ZORA calculations. Most computations on the Hg systems were carried out with two or three solvent molecules. To confirm that a fourth solvent molecule might coordinate to the heavy atom, a few examples were calculated with four solvent molecules. Up to two solvent molecules were considered for the Pt complexes.

Tables 4 and 5 list the computed Hg−C and Pt−P one-bond coupling constants for the solvated systems. In all cases, the spin−spin coupling increases substantially with increasing number of solvent molecules coordinating the heavy atom,

Table 5. Computed Pt−P One-Bond Spin−Spin Couplings K for the Solvated Compounds *cis*- and *trans*-Ptϕ_2X$_2$ (ϕ = PMe$_3$, Me = CH$_3$, X = H, Cl), in 10^{20} kg m^{-2} C^{-2}

cmpd	solvent	+ 1 solv.[a,b,c]	+ 2 solv.[a,b,c]	expt.	$\bar{R}$[c]
cis-Ptϕ_2H$_2$	acetone	⊥ 153.8		178.7[h]	3.50[f]
		∥ 155.1	∥ 169.4		
			∥ 158.3[e]		
trans-Ptϕ_2H$_2$	acetone	/ 256.8	/ 277.1	247.2[h]	3.03[g]
cis-Ptϕ_2Cl$_2$	CH$_2$Cl$_2$		325.4	331.6[i]	3.48[j]
trans-Ptϕ_2Cl$_2$	CH$_2$Cl$_2$		214.0	226.7[i]	3.48[k]

[a] Coupling constant including the number of specified solvent molecules. [b] Scalar ZORA: FC + PSO + DSO coupling, mean value of both Pt−P couplings. [c] Parallel ∥ or perpendicular ⊥ arrangement, consult text and Figure 3. See text concerning / arrangement. [d] Mean computed distance between the heavy metal and the closest solvent atoms in Å. [e] ZORA spin−orbit computation including the SD term. [f] Two solvents in ∥ arrangement, Pt−C distance. Two acetone methyl H's are close to Pt at ∼2.19 Å. [g] Pt−O distance. [h] References 57 and 58. [i] Reference 59. [j] Pt−Cl distance. Two solvent H's are close to Pt at ∼2.95 Å. [k] Pt−Cl distance. Two solvent H's are close to Pt at ∼2.59 Å.

thereby approaching the experimental values. For the Hg systems, experimental data for two different solvents are available. The experimentally observed trend for different solvents is reproduced by the computations, except for Hg(CN)$_2$, where both solvents coordinate to the Hg atom via oxygens. However, the structure with four THF molecules bound to Hg will be less favorable than the one with four methanols due to steric bulk. The solvent effect on the coupling constant is larger for stronger coordinating solvents. Spin−orbit effects can be expected to reduce the couplings as is usually the case for the unsolvated systems. We have confirmed this for Hg(CN)$_2$ and HgMeCl. In most cases, inclusion of spin−orbit effects would lead to a slighly reduced agreement with experiment. However, even the ZORA spin−orbit result for Hg(CN)$_2$ + 4 MeOH is only 3% off from experiment, a deviation which is much less than typical nonrelativistic errors for spin−spin couplings obtained with ADF.[33]

Comparing the results for the series HgMeX, X = Cl, Br, I, we find that the results for HgMeI in CHCl$_3$ are not exactly in line with the ones for HgMeCl and HgMeBr. We have observed this trend also in other calculations, showing that for similar compounds containing Cl, Br, or I the deviations of computed and experimental results are usually smaller for Cl than for I (or Br) (see e.g., Table 1). We also find slightly different solvated structures for HgMeI than for HgMeCl and HgMeBr, which leads to a somewhat different trend for increasing number of solvent molecules. Further, it might be possible that, on average, fewer solvent molecules are coordinated to HgMeI than to HgMeCl, leading to good agreement of the computed coupling with experiment for HgMeI already with three CHCl$_3$ solvent molecules. See also below for a discussion of sources of errors in our computations.

For the Pt hydride complexes, we have considered two ways by which the solvent (acetone) may bind to the Pt, as shown in Figure 3. Computations for *cis*-Ptϕ_2H$_2$ (Table 5) show that better agreement with experiment is obtained with two solvent molecules in parallel arrangement, one above and one below the square planar complex. For the perpendicular arrangement no stationary energy point was found upon geometry optimization with two acetones. The perpendicular arrangement with only one solvent was found to be about 56 kJ/mol less stable than the respective parallel one (quasi-relativistic frozen-core computations). We have only considered up to two solvents for the Pt complexes, since they complete the first coordination shell. Due to more pronounced steric bulc in the *trans*-Ptϕ_2H$_2$ complex, acetone cannot orient fully parallel to the PtP$_2$H$_2$ plane. The orientation of acetone in this complex is denoted by a / symbol in Table 5.

From Table 5 one can see that the solvent effect on the Pt complexes is similar to what we have found for the Hg compounds, resulting in a strong increase of the FC contribution to the coupling. The agreement with experiment is comparable to what has been obtained for the Hg compounds. Inclusion of solvent molecules in the computations improves the couplings substantially. Spin−orbit effects reduce the coupling constant by $\sim 10 \times 10^{20}$ kg m^{-2} C^{-2} in the solvated as well as in the unsolvated *cis*-Ptϕ_2H$_2$, leading to a less good agreement with experiment. On the other hand, spin−orbit effects can be expected to improve, for example, the coupling for *trans*-Ptϕ_2H$_2$, where the scalar ZORA value is too large. Another possibility for the overestimation of the coupling in *trans*-Ptϕ_2H$_2$ might be that there are, on average, fewer than two solvent molecules coordinated to this complex.

We cannot expect a systematic quantitative agreement with experiment from our rather simple approach since the coordination of the heavy atom in solution at finite temperature will be determined by a dynamic equilibrium of different structures. Contributions from other than the first solvent coordination shell might further be of some importance. On the other hand, the results compared to experiment are well within typical errors of the DFT approximation itself. From that we conclude that

(i) the present approach yields a reasonable description of the solvated systems. Presently neglected further solvent contributions can be expected to remain within the error range of the present computation scheme,

(ii) the average coordination of the heavy atoms is rather high, since the computations with a larger number of solvent molecules compare better with experiment in most cases, and

(iii) a sophisticated dynamical description of the solvated complexes does not seem to be necessary at the present overall level of accuracy.

Numerous approximations influence the present results, among them the use of LDA functionals in the zeroth order and in the perturbation computation as well as in the geometry optimizations, neglect of vibrational corrections in comparison with experimental data, the use of the ZORA approximation to a relativistic treatment for the spin−spin couplings, and the quasirelativistic method for the structure determination, the use of the point nucleus approximation, and the simplified description of solvent effects due to consideration of only the first coordination shell. All of them might influence the coupling constants for the studied samples by the same order of magnitude. However, for example for the TlX systems mentioned in section 2, the use of improved density functionals in the spin−spin coupling computation seems to be a crucial point.

Finally, we would like to note that, for example, a coupling constant of 147.4×10^{20} kg m^{-2} C^{-2} has been obtained earlier in ref 18 for *cis*-Ptϕ_2H$_2$ by a method being rather similar to the scaling procedure proposed in ref 14 based on nonrelativistic computations. This value is in much better agreement with the experimental coupling of 178.7×10^{20} kg m^{-2} C^{-2} than our scalar or spin−orbit ZORA computations (Table 3). However, since consideration of the solvent results in good agreement of the ZORA couplings with experiment, the scaling procedure obviously yields "better" results for the wrong reasons. It is interesting to see that the ZORA relativistic increase of the coupling constant is almost negligible for this compound, the strong relativistic effects on the atomic hyperfine integrals being

quenched by relativistic effects on the Pt−P bonds. Only with inclusion of solvent molecules the experimental value is approached. In general, ZORA computations lead to a significant improvement over the results of ref 18.

4.3. Analysis of the Solvent Effect for a Model System. The strong increase of the spin−spin coupling at the presence of solvent molecules can be explained by the coordination of the heavy atom by solvent atoms with lone pairs. The solvent will donate charge into the metal−ligand bonds, which in turn leads to an increase of the metal−ligand spin−spin coupling constants.

To gain more insight into the details of the solvent effect we have decided to study a model system: linear $Hg(CN)_2$ with two N-coordinating nucleophilic solvent molecules at an angle of 120°, the N−Hg−N coordination plane being perpendicular to the C−Hg−C axis. The solvent is represented by NH_3 at a Hg−N distance of 2.2 Å. The Hg−N distances are close to the values obtained from a geometry optimization of this system, while the $Hg(CN)_2$ bends somewhat upon optimization with two NH_3's. The change in the coupling constant due to bending of the $Hg(CN)_2$ fragment is much smaller than the solvent effect itself. This model system provides us with the features of the solvated complex without introducing too much complexity. In particular, the solvent shift will be almost quantitatively reproduced while the orbital picture remains much simpler with the N-coordinating ligands at 120° as compared to optimized structures with the O- and Cl-coordinating solvents used in the experiments. The reason it is desirable to study the solvated $Hg(CN)_2$ at the same geometry as the free molecule is that the ADF program can provide a convenient decomposition of the molecular orbitals (MOs) of the solvated complex in terms of the MOs of the building fragments (fragment MOs = FOs). By choosing the entire unsolvated $Hg(CN)_2$ as a fragment, we can trace the orbital contributions to the spin−spin couplings in the solvated system back to the respective positive and negative orbital contributions of the unsolvated system. The FOs themselves can further be expressed in terms of the constituting atomic orbitals (AOs). We restrict the following discussion to the scalar relativistic FC contribution.

Orbital contributions to the coupling constant arise intuitively (but somewhat arbitrarily) from the summation over the occupied Kohn−Sham orbitals in eq 3. We choose this subdivision of the coupling constant for the following analysis.

It has been argued elsewhere,[9,12] that the core orbitals of the heavy atom will have no or almost no influence on the coupling constants, since an orbital must have rather large electron density close to *both* of the involved nuclei. See also eq 6 below. For the free $Hg(CN)_2$ fragment we find only four major contributions from valence σ FOs to the Hg−C coupling. The respective orbitals are displayed in Figure 4 together with their individual contributions. The four terms sum up to 441×10^{20} kg m^{-2} C^{-2}, which is very close to the total FC coupling of 444×10^{20} kg m^{-2} C^{-2}, Table 2.

In the usual picture of orthogonal canonical Kohn−Sham FOs, the coupling is determined by huge positive contributions from Hg−C bonding FOs, which are to a large extent canceled by a negative contribution from a Hg−C antibonding FO. Since a unitary transformation of the Kohn−Sham orbitals does not change the one-determinantal wave function of the noninteracting system and therefore not the true electron density density, we can for example choose the orbitals being localized in order to provide an alternative picture of bonding. Localized linear combinations (LFOs) of the occupied σ orbitals of Figure 4 are displayed in Figure 5 together with their percentage composition

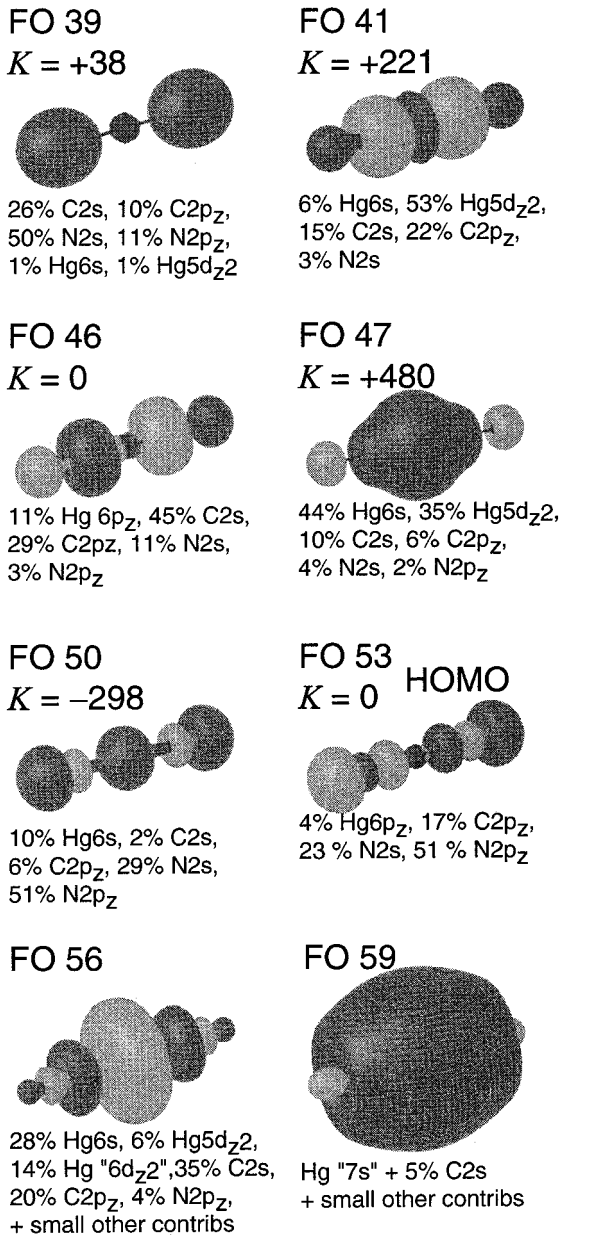

Figure 4. Valence σ orbitals for the $Hg(CN)_2$ fragment and their contribution to the Hg−C spin−spin coupling in 10^{20} kg m^{-2} C^{-2}. The numbering refers to an ADF computation without employing symmetry. The percentages for C and N refer to the contributions of both atoms. FO 40 is the σ_u analogue of FO 39. Two unoccupied orbitals are shown as well. The molecule is oriented along the *z*-axis.

of each FO of Figure 4. The respective Boys−Foster[65] orbital localization and a population analysis of localized orbitals in terms of fragment orbitals has earlier been implemented into ADF by one of the authors (J.A.). From Figure 5 one can see that there are three LFOs which consist, to a large extent, of the strongly positively contributing FOs. Two of them obviously represent the Hg−C σ bonds (Figure 5B), while the third one is a Hg-5d$_\sigma$-6s hybrid which has also some Hg−C bonding character (Figure 5A). The remaining LFOs represent the C−N σ bonds (Figure 5C) and the N lone pairs (Figure 5D). The strongly negatively contributing FO 50 is somewhat distributed

(64) Goggin, P. L.; Goodfellow, R. J.; McEwan, D. M.; Griffiths, A. J.; Kessler, K. *J. Chem. Res.* **1979**, *M*, 2315.

(65) (a) Boys, S. F.; Foster, J. M. *Rev. Mod. Phys.* **1960**, *32*, 300. (b) Boys, S. F. In *Quantum Theory of Atoms, Molecules and the Solid State*; Löwdin, P. O., Ed.; Academic Press: New York, 1966, p. 253.

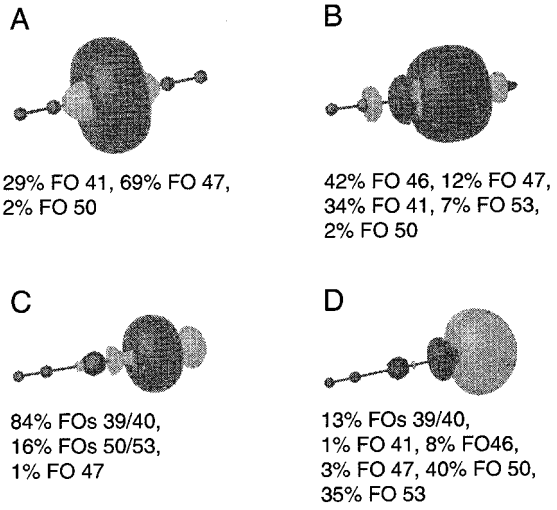

Figure 5. Localized valence orbitals for the $Hg(CN)_2$ fragment. (A) a Hg6s−Hg5d$_{z^2}$ hybrid with contributions from the carbons, (B) one of the two Hg−C σ bonds, (C) one of the two C−N σ bonds, (D) one of the two N lone pairs. See section 4.3 and Figure 4.

over LFOs which are also composed of positively contributing FOs. In some sense, the localized picture seems to provide a description with less pronounced cancellation of positive and negative terms. The coupling is determined—as expected—by the Hg−C σ bonds. However, by choosing the orbitals to be *orthogonal*, as is the case here, counterintuitive contributions to the Hg−C couplings for example from the C−N σ bonds and the N lone pair (L)FOs must occur because of their orthogonalization tails at the Hg and C nuclei.

Figure 6 displays the MOs in the solvated model complex which contribute to the Hg−C spin−spin couplings. The individual terms sum up to 522×10^{20} kg m^{-2} C^{-2}, reflecting the substantial shift of the FC coupling due to a solvent. The result is quite similar to the couplings obtained with two MeOH or THF solvents, Table 4. Two of the MOs (MO 43, MO 45) are essentially $Hg(CN)_2$ FOs (FO 39, FO 41), with almost the same contributions to the coupling. Since the linear symmetry of the $Hg(CN)_2$ fragment is destroyed in the solvated complex, σ, π, and δ $Hg(CN)_2$ FOs can mix with solvent FOs. The positively contributing FO 47 (Figure 4) is contained in the positively contributing MOs 51, 54, and 63. The negative contributions of MOs 57 and 58 can be understood by their partial composition of FO 50. Antibonding interaction of FO 50 with the solvent FOs reduces its Hg−C antibonding character, resulting in a rather small magnitude of the total negative contributions. MO 63, which contains a large part of FO 47, also consists of virtual σ* FOs, which mix with the solvent lone pair FOs. This MO yields a huge positive contribution to the Hg−C coupling.

By expanding the first-order perturbed MOs of eq 3 in the basis of occupied and virtual unperturbed MOs, the FC coupling constant can be written as

$$K(\mathrm{A,B}) = \frac{2}{3} \sum_{k=x,y,z} \sum_{i}^{\mathrm{occ}} \sum_{a}^{\mathrm{virt}} \frac{\langle a|\hat{O}_{\mathrm{A}k}|i\rangle\langle i|\hat{O}_{\mathrm{B}k}|a\rangle}{\epsilon_i - \epsilon_a} \qquad (6)$$

where i and a are the real scalar relativistic unperturbed occupied (occ) or unoccupied (virt) MOs, and $\hat{O}_{\mathrm{A}k}$, $\hat{O}_{\mathrm{B}k}$ are the Fermi-contact perturbation operators (including the first-order potential change due to the induced spin-density) for k-direction for the two nuclei. The ϵ's are the orbital energies. For the $Hg(CN)_2$ fragment, we find that major parts of the positive contributions

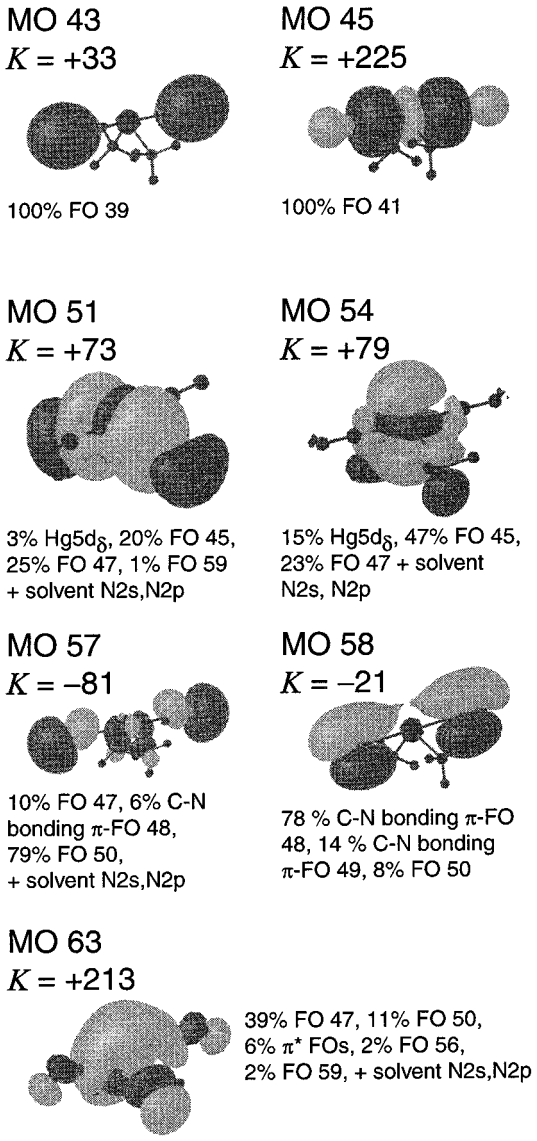

Figure 6. Valence orbitals of $Hg(CN)_2 + 2\ NH_3$ which contribute to the Hg−C spin−spin coupling, and their composition of fragment orbitals, Figure 4. The numbering refers to the ADF computation. Coupling contributions in 10^{20} kg m^{-2} C^{-2}. See section 4.3.

to the FC term come from coupling of occupied FO $i = 47$ with virtual FO $a = 56$ 481×10^{20} kg m^{-2} C^{-2} + small positive and negative contributions from coupling with other virtual FOs which sum up to -1×10^{20} kg m^{-2} C^{-2}) and occupied FO 41 with virtual FO 56 (211×10^{20} kg m^{-2} C^{-2}). The negative contribution of FO 50 also originates in coupling with virtual FO 56 (-288×10^{20} kg m^{-2} C^{-2}). The virtual σ FOs $a = 56$ and 59 are partially populated (Mulliken gross populations of 0.05 and 0.07, respectively) in the solvated system, thereby increasing the electron density at the mercury atom and in particular in the Hg−C bond. The Mulliken charges for Hg, C and N in the $Hg(CN)_2$ fragment are +0.56, −0.09, and −0.19, respectively. The Hirshfeld charges are +0.61, −0.11, and −0.19, in reasonable agreement with the Mulliken charges. The Hg−C overlap populations are 0.58. In the solvated complex, we obtain Mulliken charges for the $Hg(CN)_2$ fragment of +0.38, −0.12, and −0.27, for Hg, C, and N, respectively (Hirshfeld charges: +0.37, −0.17, −0.24). This clearly indicates the increase of electron density at both the Hg and the C atoms. Also, the Hg−C overlap populations rise to 0.67. Charge donation by the solvent increases the electron density at the

Hg and C atoms and in the Hg−C bond, which is responsible for the substantial increase of the nuclear spin−spin coupling between Hg and C at the presence of solvent molecules.

Relative magnitudes of spin−spin couplings are often explained by the hybridization of the coupled atoms. We do not follow this approach here. The concept of hybridization within the MO model deals with the question of *which* atomic orbitals are mixed in order to form a molecular orbital (e.g., s and $p_z \rightarrow$ sp, s and p_x, p_y, $p_z \rightarrow sp^3$), while the magnitude of the coupling constant is determined by the respective *amount* of (here: s-) contribution in the bonding MOs. In rather simple cases the hybridization type can serve as a guidance to the amount of s-character in a bond. An example might be a comparison of the Hg−C coupling in $Hg(CN)_2$ and $[Hg(CN)_4]^{2-}$, for which the coupling in the tetrahedral complex is, as expected, much smaller as in the linear complex. See Figure 1. From our analysis in this section it becomes clear, though, that an equal amount of the difference between the Hg−C couplings in the two complexes is due to solvent effects.

5. Conclusions

We could demonstrate that solvent effects on heavy atom NMR spin−spin coupling constants can be very substantial. Density functional computations of a number of solvated Hg and Pt complexes yield reasonable agreement with experimental data obtained from solution. Charge donation by the solvent to the coordinated heavy atom and into the heavy atom−ligand bonds plays an important role for the large increase of the Fermi-contact contribution to the coupling constants. Therefore, solvent molecules have to be explicitly taken into account. The resulting overall accuracy of the ZORA relativistic density functional computations is comparable to or better than those of nonrelativistic computations for unsolvated light atomic systems obtained earlier with ADF.[9,33] Spin−orbit effects as well as the influence of the spin−dipole term turn out to be rather small for this particular set of samples, compared to scalar relativistic and solvent effects on the Fermi-contact contribution.

Our analysis shows that for the investigated cases solvent effects represent a major influence concerning experimentally determined spin−spin couplings. We propose that solvent effects might be of minor importance in a qualitative discussion of metal−ligand couplings of coordinatively saturated compounds, while they will be substantial for metal−ligand coupling constants of coordinatively unsaturated heavy metal compounds. Especially in a comparison of couplings between coordinatively saturated and unsaturated systems solvent effects should be considered even at a qualitative level.

Acknowledgment. This work has received financial support from the National Science and Engineering Research Council of Canada (NSERC).

JA003481V